Analysis of the build-up of polyurethane networks from toluenediisocyanate and castor oil considering intra-molecular reactions

Stella M. Moschiar, C. A. L. Piacentini and Roberto J. J. Williams*
Institute of Materials Science and Technology (INTEMA), University of Mar del Plata and National Research Council (CONICET), J. B. Justo 4302, (7600) Mar del Plata, Argentina
(Received 5 August 1987; revised 5 October 1987; accepted 12 October 1987)

The build-up of polyurethane networks prepared by reacting toluenediisocyanate (TDI 80:20) with an excess of castor oil over the stoichiometric balance has been analysed using a fragment approach. This includes a kinetic scheme giving the evolution of the different species and fragments into which the network may be divided together with a recursive method to obtain statistical parameters. Intra-molecular reactions leading to the smallest cycles are taken into account in the analysis. Sol fraction and concentration of elastically active network chains in the gel fraction are estimated as a function of the stoichiometric imbalance and compared with experimental results previously reported. A reasonable fit is shown for an effective bond length in the smallest cycle equal to 0.23 nm.

(Keywords: polyurethanes; toluenediisocyanate; castor oil; networks; statistics; cyclization; intra-molecular reactions)

INTRODUCTION

Polyurethane networks prepared by reacting toluenediisocyanate (TDI 80:20) with an excess of castor oil over the stoichiometric balance have been described in a previous paper[1]. Their characterization involved the determination of the glass transition temperature (TMA), the sol fraction, w_s (extraction with toluene), and the concentration of elastically active network chains, EANC (swelling in benzene). The observed experimental trends of w_s and EANC as a function of the stoichiometric imbalance were predicted by statistical calculations. However, a systematic deviation, i.e. w_s (exp.) $>$ w_s (predicted), suggested that intra-molecular reactions, not considered in the ideal polymerization scheme, were effectively taking place.

Our aim is to re-analyse this polymerization by taking into account the possibility of the formation of the smallest intra-molecular cycles between TDI residues and OH functionalities belonging to the same castor oil molecule. A fragment approach, which has been successfully used for several non-ideal polymerizations, such as the production of phenolics[2,3], the build-up of epoxy-amine networks with simultaneous polyetherification[4], and the build-up of polymer networks by initiated polyreactions[5], will be used to analyse the effect of the smallest cycles. Predictions will be compared with reported experimental results[1].

IDENTIFICATION OF FRAGMENTS

Figure 1 shows the notation for the molecular species present in the initial reaction mixture and *Figure 2* indicates the chemical formula of two of them.

Castor oil is an ester of glycerine with several fatty acids, including approximately 90% ricinoleic acid, as determined by gas chromatography. Ricinoleic acid has a secondary OH group that reacts with the NCO groups of TDI, forming the polyurethane network. Assuming a random esterification, the probability that any one of the three fatty acids of a castor oil molecule is ricinoleic acid is 0.9. Then the initial molar concentration of each species of castor oil is:

$$\begin{aligned} A_0(0) &= (0.1)^3 A = 0.001 A \\ A_2(0) &= (0.9)^3 A = 0.729 A \\ A_3(0) &= 3(0.9)^2(0.1) A = 0.243 A \\ A_4(0) &= 3(0.9)(0.1)^2 A = 0.027 A \end{aligned} \quad (1)$$

where $A = A_0(0) + A_2(0) + A_3(0) + A_4(0)$ is the initial molar concentration of castor oil.

The number average functionality of castor oil molecules is given by

$$f_n = 0[A_0(0)/A] + 1[A_4(0)/A] + 2[A_3(0)/A] + 3[A_2(0)/A] = 2.7 \quad (2)$$

The reactivities of *o*-NCO and *p*-NCO of the 2,4 TDI molecule are not the same, but their difference decreases as temperature increases[6]. However, as networks have a stoichiometric excess of castor oil, i.e. $r < 1$, and NCO functionalities are reacted to completion, the difference in reactivity will not affect significantly the fraction of intra-molecular cycles and the corresponding properties of the resulting material. Thus no distinction between *o*- and *p*-NCO functionalities has been made in the notation shown in *Figure 1*.

---

*To whom all correspondence should be addressed

0032-3861/88/050914-05$03.00

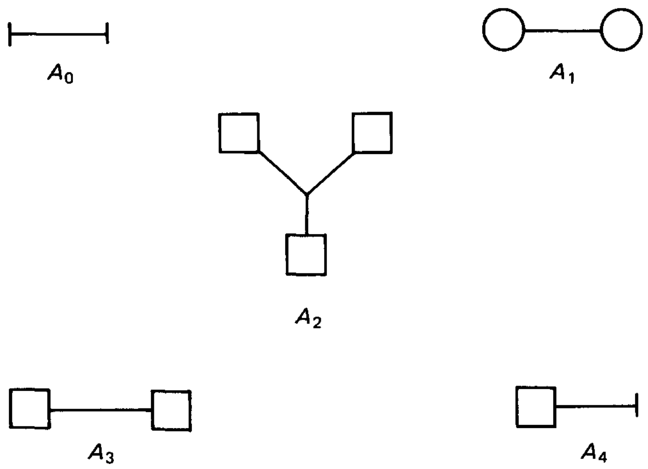

Figure 1 Initial molecular species: A_0, castor oil molecule esterified with acids other than ricinoleic (no OH functionality); A_1, toluenediisocyanate; A_2, castor oil esterified with three ricinoleic acid molecules (trifunctional); A_3, castor oil esterified with two ricinoleic acid molecules (bifunctional); A_4, castor oil esterified with one ricinoleic acid molecule (monofunctional)

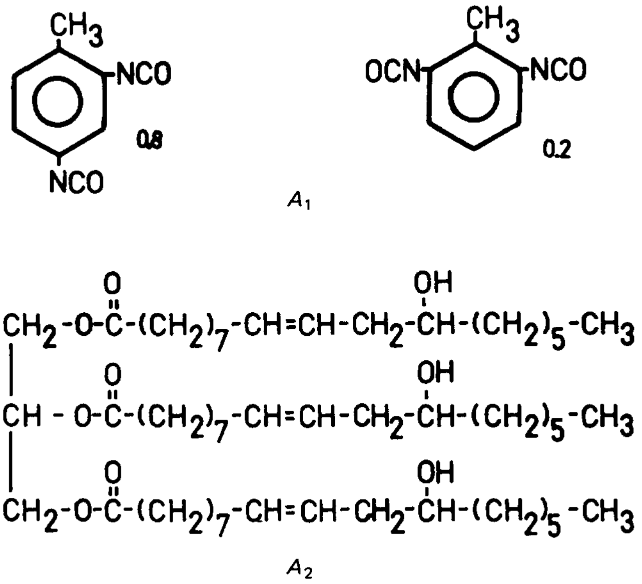

Figure 2 Chemical structures of species A_1 and A_2

The stoichiometric imbalance is defined as

$$r = 2\,A_1(0)/2.7\,A \qquad (3)$$

Figure 3 shows the different species and fragments that appear during the polymerization. A_5 is the product of reacting one OH functionality of an A_2 molecule with an NCO group of an A_1 molecule (full squares and circles represent reacted functionalities). When the free NCO present in the A_5 molecule reacts with an OH pertaining to another molecule, it gives place to A_6 and A_7 (+ bonds are joined to − bonds when generating the network). When the same free NCO of A_5 reacts intra-molecularly it leads to A_8. Structures A_9–A_{17} represent the remaining possibilities arising from the reaction of A_2. Similarly, A_{18}–A_{23} are the possible structures obtained from A_3, while A_{24} and A_{25} are those resulting from A_4.

At the end of reaction, all free NCO groups will disappear from the reaction mixture. Thus, at full conversion, the concentrations of A_1, A_5, A_9, A_{10}, A_{12}, A_{14}, A_{15}, A_{16}, A_{18}, A_{21}, A_{22} and A_{24} will be zero. In these conditions, the only cyclic structures will be A_8, A_{13} and A_{19}. While A_8 and A_{19} will be part of the sol, A_{13} may belong to the sol or may be the extreme of a pendant chain of the gel. This will depend on the probability of having a finite (or an infinite) chain when looking out from a + bond.

Only the smallest cycles are considered in this first-order analysis. According to the chemical structures shown in *Figure 2*, these cycles are composed of two ricinoleic acid arms and one TDI residue, giving a total number of bonds $\nu = 37.5$ (37 for two neighbouring and 38 for two extreme ricinoleic acid arms of the castor oil molecule). The probability of forming larger cycles, i.e. involving i times the units necessary to build up the smallest cycle ($i = 2, 3, \ldots$), decreases as $i^{3/2}$, as discussed by Stepto[7].

KINETIC SCHEME

Inter-molecular steps are taken as second-order reactions while intra-molecular steps are taken as first-order reactions, with specific rate constants k and k_c, respectively. These rate constants refer to a couple of reaction sites. Thus the rate constant for the reaction between A_1 and A_2 is $6k$, while the intra-molecular reaction in A_9 has a rate constant equal to $2k_c$.

A balance for every species and fragment may be written starting from the kinetic scheme. For example, the rate of generation of the cyclic fragment A_{13} is given by

$$\begin{aligned} dA_{13}/dt = {} & k_c A_{10} + kA_8(A_5 + 2A_9 + A_{10} + 2A_{12} + 3A_{14} \\ & + 2A_{15} + A_{16} + A_{18} + 2A_{21} + A_{22} + A_{24}) \\ & + kA_{12}(3A_2 + 2A_3 + A_4 + 2A_5 + 2A_6 + A_9 \\ & + A_{10} + A_{11} + A_{18} + A_{20}) \end{aligned} \qquad (4)$$

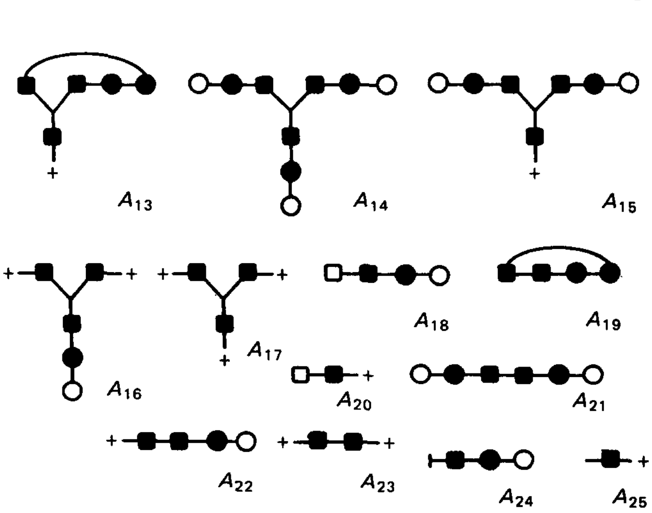

Figure 3 Species and fragments generated during the polymerization

By defining $A_i^* = A_i/A_1(0)$ (for $i=1, \ldots, 25$), and $t^* = kA_1(0)t$, equation (4) may be written as

$$\begin{aligned} \mathrm{d}A_{13}^*/\mathrm{d}t^* = {} & K_c A_{10}^* + A_8^*(A_5^* + 2A_9^* + A_{10}^* + 2A_{12}^* + 3A_{14}^* \\ & + 2A_{15}^* + A_{16}^* + A_{18}^* + 2A_{21}^* + A_{22}^* + A_{24}^*) \\ & + A_{12}^*(3A_2^* + 2A_3^* + A_4^* + 2A_5^* + 2A_6^* + A_9^* + \\ & + A_{10}^* + A_{11}^* + A_{18}^* + A_{20}^*) \end{aligned} \tag{5}$$

where

$$K_c = k_c/kA_1(0) \tag{6}$$

is a dimensionless group that characterizes the significance of the intra-molecular reaction.

For a Gaussian chain, the ratio k_c/k for the formation of the smallest cycle is given by[7]

$$k_c/k = (3/2\pi \nu b^2)^{3/2}(1/N) \tag{7}$$

where b is the effective bond length and N is the Avogadro number.

Balances similar to equation (5) were written for the remaining species and fragments and solved using a fourth-order Runge–Kutta method until a conversion of NCO groups higher than 0.999999, for $r \leqslant 0.9$, and 0.9999, for $r > 0.9$, was attained (the reaction was carried out to completion for practical purposes). The conversion of NCO functionalities is defined as

$$\begin{aligned} p_{\mathrm{NCO}} = 1 - 0.5(& 2A_1^* + A_5^* + 2A_9^* + A_{10}^* + A_{12}^* + 3A_{14}^* + 2A_{15}^* \\ & + A_{16}^* + A_{18}^* + 2A_{21}^* + A_{22}^* + A_{24}^*) \end{aligned} \tag{8}$$

The initial dimensionless concentrations were obtained from the selected value of the stoichiometric imbalance, r. Thus, $A_1^*(0) = 1$, $A^*(0) = 2/2.7r$, $A_0^*(0) = 0.001\,A^*(0)$, $A_2^*(0) = 0.729\,A^*(0)$, $A_3^*(0) = 0.243\,A^*(0)$, $A_4^*(0) = 0.027\,A^*(0)$, $A_5^*(0), \ldots, A_{25}^*(0) = 0$. On the other hand, the dimensionless parameter K_c was calculated by using k_c/k (mol l^{-1}) as an adjustable parameter, and $A_1(0)$ as the actual value for the selected r. Taking into account that the densities of the reactants are $\rho_{\mathrm{TDI}} = 1.222$ g ml^{-1}, $\rho_{\mathrm{castor\,oil}} = 0.959$ g ml^{-1}, and the molecular weights are $M_{\mathrm{TDI}} = 174$ g mol^{-1}, $M_{\mathrm{castor\,oil}} = 928.4$ g mol^{-1}, and using equation (3), we get the following expression for $A_1(0)$:

$$A_1(0)\ (\mathrm{mol\,l^{-1}}) = r/(0.7171 + 0.1424\,r) \tag{9}$$

Figure 4 shows the fraction of cyclic species at the end of polymerization, for $k_c/k = 0.2$ mol l^{-1}. This particular value gave the best agreement between theory and experiment, as is shown below. The fractions of both $A_2(0)$ and $A_3(0)$ forming intra-molecular cycles increase when the system approaches stoichiometry ($r = 1$). This is the expected trend for intra-molecular reactions in a random polymerization[7]. The decrease of A_8 with r is due to the corresponding increase in its conversion to A_{13} when approaching stoichiometry. The fraction $A_{13}/A_2(0)$ is higher than $A_{19}/A_3(0)$, for every stoichiometric imbalance, because of the higher probability of forming a cycle in a trifunctional molecule than in a bifunctional one.

STATISTICS OF NETWORK FORMATION

To compare theoretical predictions with experimental results[1] of the sol fraction, w_s, and the EANC concentration, only post-gel properties are of interest. Let us call T_P and T_N the probabilities of finding a finite chain leaving a particular fragment from a + bond and a − bond, respectively. These probabilites are calculated as

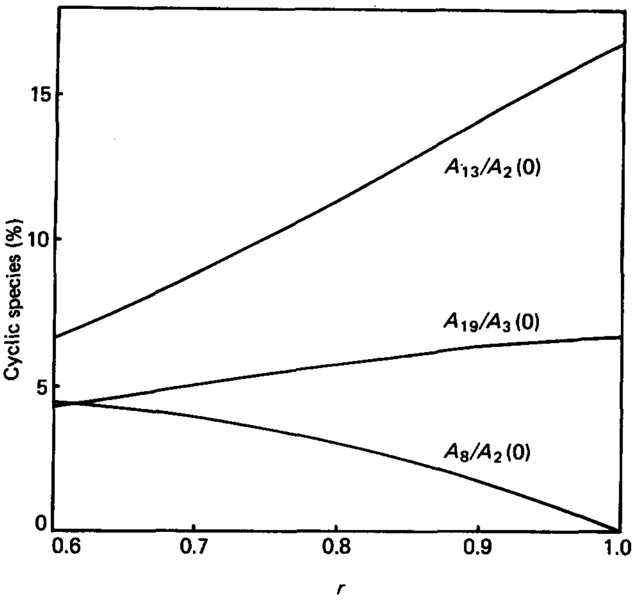

Figure 4 Fraction of cyclic species at the end of polymerization, as a function of the stoichiometric imbalance for $k_c/k = 0.2$ mol l^{-1}

$T_P = \sum_{\text{fragments}}$ (fraction of total − bonds associated with a particular fragment) × (probability that all branches leaving the fragment, already joined by a + bond, are finite) (10)

$T_N = \sum_{\text{fragments}}$ (fraction of total + bonds associated with a particular fragment) × (probability that all branches leaving the fragment, already joined by a − bond, are finite) (11)

As the total number of + bonds is equal to the number of − bonds (a condition implicit in the reaction·scheme), at the end of reaction, i.e. when $A_1 = A_5 = A_9 = A_{10} = A_{12} = A_{14} = A_{15} = A_{16} = A_{18} = A_{21} = A_{22} = A_{24} = 0$, it is verified that

$$2A_7 = A_6 + 2A_{11} + A_{13} + 3A_{17} + A_{20} + 2A_{23} + A_{25} \tag{12}$$

Then

$$T_P = (1/2A_7)2A_7T_N = T_N \tag{13}$$

$$\begin{aligned} T_N = (1/2A_7)(& A_6 + 2A_{11}T_P + A_{13} + 3A_{17}T_P^2 + A_{20} + 2A_{23}T_P \\ & + A_{25}) \end{aligned} \tag{14}$$

From equations (13) and (14), and using dimensionless concentrations, we get

$$T_P = [-b - (b^2 - 4ac)^{1/2}]/2a \tag{15}$$

where $a = 3A_{17}^*$, $b = 2(A_{11}^* + A_{23}^* - A_7^*)$, $c = A_6^* + A_{13}^* + A_{20}^* + A_{25}^*$.

Sol fraction

To calculate the sol fraction we need to determine the mass fraction of the fragments remaining at the end of polymerization. The total mass per initial mol of A_1 is given by

$$m_T/A_1(0)=M_1+2M/2.7r \qquad (16)$$

where $M_1=174\,\mathrm{g\,mol^{-1}}$ is the molecular mass of TDI and $M=928.4\,\mathrm{g\,mol^{-1}}$ is the molecular mass of castor oil.

The mass fraction of a generic fragment A_i ($i=0, \ldots, 25$) is calculated as

$$W_i=A_i^* M_i/(M_1+2M/2.7r) \qquad (17)$$

where $M_0=M_2=M_3=M_4=M_6=M_{11}=M_{17}=M_{20}=M_{23}=M_{25}=M$; $M_7=174$; $M_8=M_{13}=M_{19}=1102.4$. It has been assumed that the molecular mass of fragments arising from castor oil does not change with the fatty acid composition or with the hydrogen abstraction to form the urethane linkage.

The sol fraction of the material, at the end of polymerization, is given by

$$w_s=W_0+W_2+W_3+W_4+W_6T_P+W_7T_P^2+W_8+W_{11}T_P^2+W_{13}T_P+W_{17}T_P^3+W_{19}+W_{20}T_P+W_{23}T_P^2+W_{25}T_P \qquad (18)$$

Concentration of elastically active network chains

The concentration of crosslinking units per unit mass with three branches going to the gel, X_3, may be calculated as

$$X_3=\{A_{17}^*/[m_T/A_1(0)]\}(1-T_P)^3 \qquad (19)$$

Substituting for $m_T/A_1(0)$ from equation (16) into equation (19), we get

$$X_3=[A_{17}^*/(M_1+2M/2.7r)](1-T_P)^3 \qquad (20)$$

The EANC concentration per unit mass is given by

$$\mathrm{EANC}\ (\mathrm{mol\ g^{-1}})=(3/2)X_3 \qquad (21)$$

To compare theoretical predictions with experimental results it is convenient to express the EANC concentration per unit volume of gel, i.e. material deprived of the sol fraction. The necessary transformation is

$$\mathrm{EANC}\ (\mathrm{mol\ cm^{-3}})=(3/2)X_3\rho_{\mathrm{gel}}/(1-w_s) \qquad (22)$$

where w_s is obtained from equation (18) and experimental values of densities of gel fractions, ρ_{gel}, are available[1].

RESULTS AND DISCUSSION

Polyurethane networks were prepared using stoichiometric imbalances, r, ranging from 0.6 to 1. Reaction conditions were such that NCO groups were exhausted as shown by i.r. (typical conditions were 48 h at 60°C)[1]. The sol fraction was obtained by extraction with toluene in a Soxhlet device. The EANC concentration was calculated from the swelling data of the gel fraction in benzene, assuming two different limits: affine deformation and phantom network deformation. These experimental results have been reported elsewhere[1].

Figure 5 shows experimental and predicted values of the sol fraction as a function of the stoichiometric imbalance. For $k_c/k=0.2\,\mathrm{mol\,l^{-1}}$ a reasonable agreement is obtained, in contrast to the prediction assuming that no intra-molecular reactions take place ($k_c=0$).

Figure 6 shows experimental and predicted curves for the EANC concentration in the gel. According to the network deformation model used to interpret the set of experimental data, two limiting curves arise: one for affine deformation and the other for phantom network deformation. The predicted curve for $k_c/k=0.2\,\mathrm{mol\,l^{-1}}$

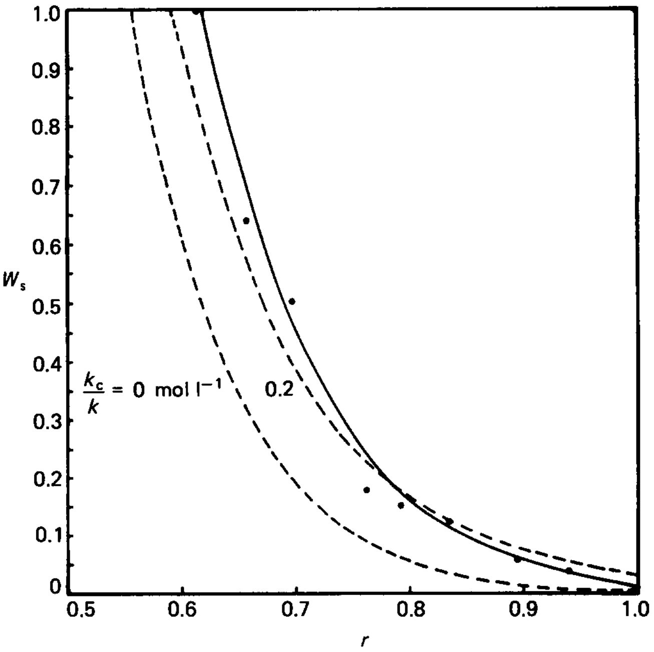

Figure 5 Experimental (full line) and predicted (dashed line) values of the sol fraction as a function of the stoichiometric imbalance

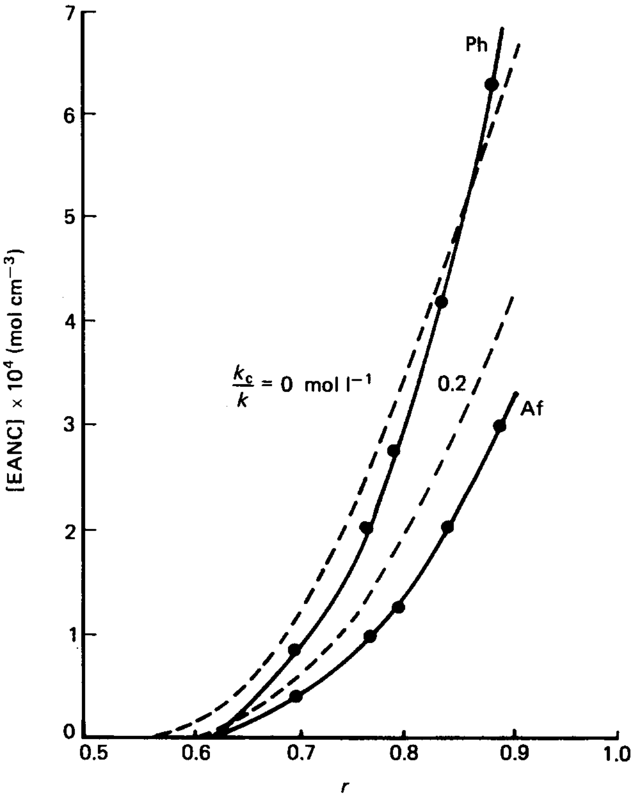

Figure 6 Experimental EANC concentration in the gel (full lines), for the two limits of network deformation (Af, affine; Ph, phantom), compared with predicted values (dashed lines), as a function of the stoichiometric imbalance

lies between the two possibilities. When cyclization reactions are neglected, the predicted curve, for low values of the stoichiometric imbalance *r*, lies outside the expected range.

The effective bond length calculated from equation (7), using $k_c/k = 0.2 \text{ mol l}^{-1}$, is $b = 0.23$ nm. This value may be compared with corresponding *b* values for polymethylene and polyoxyethylene chains, namely 0.40 and 0.29 nm, respectively[7]. The fact that the value of *b* arising from the best fit lies in the expected range adds weight to the validity of the present analysis.

Moreover, this paper together with previous ones[2-5] shows the simplicity of the fragment approach in dealing with non-ideal polymerizations, i.e. presence of several competing reactions, unequal reactivity of functionalities, substitution effects and formation of intra-molecular cycles.

REFERENCES

1 Cuadrado, T. R. and Williams, R. J. J. *Makromol. Chem. Macromol. Symp.* 1986, **2**, 61

2 Aranguren, M. I., Borrajo, J. and Williams, R. J. J. *Ind. Eng. Chem. Prod. Res. Dev.* 1984, **23**, 370

3 Vázquez, A., Adabbo, H. E. and Williams, R. J. J. *Ind. Eng. Chem. Prod. Res. Dev.* 1984, **23**, 375

4 Riccardi, C. C. and Williams, R. J. J. *Polymer* 1986, **27**, 913

5 Williams, R. J. J., Riccardi, C. C. and Dušek, K. *Polym. Bull.* 1987, **17**, 515

6 Aranguren, M. I. and Williams, R. J. J. *Polymer* 1986, **27**, 425

7 Stepto, R. F. T. in 'Developments in Polymerisation—3' (Ed. R. N. Haward), Applied Science, London, 1982, pp. 81–141 (and references therein)